IAEA
International Atomic Energy Agency

20th IAEA Fusion Energy Conference
Vilamoura, Portugal, 1-6 November 2004

IAEA-CN-116/FT/P7-8

Design Study of National Centralized Tokamak Facility for the Demonstration of Steady State High Beta Plasma Operation

H. Tamai[1)], and the National Centralized Tokamak Facility Design Team*
Naka Fusion Research Establishment, Japan Atomic Energy Research Institute, Mukoyama, Naka-machi, Ibaraki-ken, 311-0193 Japan
E-mail:tamai@naka.jaeri.go.jp

*** the National Centralized Tokamak Facility Design Team**
N. Yoshida[2)], H. Azechi[3)], K. Ida[4)], T. Imai[5)], M. Ichimura[5)], Y. Uesugi[6)], K. Okano[7)], A. Kimura[8)], M. Sakamoto[2)], A. Sagara[4)], R. Shimada[9)], A. Shimizu[2)], S. Tanaka[10)], K. Nakamura[2)], A. Nishimura[4)], H. Hashizume[11)], H. Horiike[3)], M. Matsuoka[12)], Y.-M Miura[3)], M. Akiba[1)], K. Okuno[1)], H. Kubo[1)], K. Kurihara[1)], S. Sakurai[1)], K. Masaki[1)], M. Matsukawa[1)], N. Miya[1)], Y. Miura[1)], Y. Takase[10)], T. Hino[13)], A. Kohyama[8)], H. Ninomiya[1)], M. Kikuchi[1)], M. Kuriyama[1)], N. Hosogane[1)], Y. Kamada[1)], H. Takatsu[1)], K. Yatsu[5)], S. Itoh[2)], N. Inoue[10)], M. Fujiwara[4)], T. Fujita[1)], G. Kurita[1)], H. Kawashima[1)], K. Tsuchiya[1)], A. Morioka[1)], K. Kizu[1)], Y. Kudo[1)], N. Hayashi[1)], M. Takechi[1)], T. Suzuki[1)], A. Isayama[1)], K. Hamamatsu[1)]

[2)]Kyushu Univ., [3)]Osaka Univ., [4)]National Institute of Fusion Science, [5)]Univ. of Tsukuba, [6)]Kanazawa Univ., [7)]Central Research Institute of Electric Power Industry, [8)]Kyoto Univ., [9)]Tokyo Institute of Technology, [10)]Univ of Tokyo, [11)]Tohoku Univ., [12)]Mie Univ., [13)]Hokkaido Univ.

Design Study of National Centralized Tokamak Facility for the Demonstration of Steady State High Beta Plasma Operation

H. Tamai, and the National Centralized Tokamak Facility Design Team

Naka Fusion Research Establishment, Japan Atomic Energy Research Institute,
Mukoyama, Naka-machi, Naka-gun, Ibaraki-ken, 311-0193 Japan

E-mail: tamai@naka.jaeri.go.jp

Abstract. Design studies are shown on the National Centralized Tokamak facility (formerly called JT-60SC). The machine design is performed to extend the flexibility in aspect ratio and shape controllability for the demonstration of the high-β steady state operation with nation-wide collaboration, in parallel with ITER towards DEMO. Increasing shape parameter S [$\equiv q_{95}I_p/a_pB_T \sim A^{-1}\{1+\kappa^2(1+2\delta^2)\}$] ~7 is expected by the low aspect ratio of A~2.6 as well as high elongation of κ_{95}~1.9. Physics investigation shows that the advantage of low aspect ratio configuration in improvement of MHD stability. Break-even-class plasma performance, and capability to sustain non-inductively driven high beta plasma (βN=3.5-5.5) for more than 100 second are also estimated to be marginally satisfied.

1. Introduction

The demonstration of high beta steady-state operation is an important element of tokamak research for a future tokamak reactor [1] to be an economically viable energy system. Aimed at an improvement of tokamak concept for early realization of fusion energy, the former JT-60 superconducting modification project (JT-60SC) [2] is adjusted to widen operation regime of high beta steady-state research named as the 'National Centralized Tokamak (NCT) facility program' to be progressed under nation-wide collaborations with universities, research institutes, and industries. The design requirements set by nation-wide discussion are, 1) a super-conducting device with break-even-class plasma performance, 2) capability of steady state high-β (β_N=3.5-5.5) plasma with full non-inductive current drive, required for the DEMO for more than 100 second, 3) to provide mobility and flexibility in terms of plasma aspect ratio, plasma shaping control, and feedback control.

First requirement is set to enable small normalized gyroradius ($\rho^* << 1/100$) experiment at low collisionality ($\nu^* << 1$) for the best contribution to DEMO and ITER physics. Second requirement is marginally met by the present heating and current drive systems in JT-60U if the pulse length is extended. Third requirement is significantly modified compared with previous design to increase beta limit through the extension of flexibility in shaping and aspect ratio.

This paper presents the machine design and physics investigation of NCT in the viewpoint of the flexibility extension in aspect ratio and plasma shape for the demonstration of steady state high beta plasma operation, and the prpgress in technical design and R&D activity.

2. Design Optimization towards the Extension of Flexibility

Configuration optimization is one of important research elements to achieve high beta steady-state operation. DIII-D experiments show that higher beta operation becomes possible

by increasing so-called shape parameter $S \equiv q_{95}I_p/a_pB_T \sim A^{-1}\{1+\kappa^2(1+2\delta^2)\}$ through aspect ratio, elongation and triangularity controls [3]. In DIII-D shape parameter up to 7.4 is achieved by the shape optimization with κ=2.0 and δ=0.9. Design of NCT aims at achieving higher shape parameter in combination with the aspect ratio as well as plasma shaping (κ, δ). In order to characterize the NCT, parameter range of the aspect ratio is settled at that with much difference from ITER [4]. Another importance is the consistency with recent design of DEMO, in which the feasibility of compact size with low aspect ratio is precisely investigated due to the economical advantage. With those considerations, aspect ratio of NCT is extended to 2.6.

In order to achieve a high shape parameter, elongation should be high at the same time. However, the consistency of such a high elongation plasma with a high performance divertor for particle pumping and heat removal is often kept as open question. In NCT design, vertical elongation is optimized to ensure the divertor geometry for pumping speed and leg length enough to sustain the divertor detachment [5].

3. Machine Design to Satisfy the Required Condition

Design studies have been made to increase operational flexibility on the plasma aspect ratio, and the controllability of plasma shaping.

The design study has started from the previous design of JT-60SC, presented at IAEA FEC 2002 [1]. In new design the present JT-60U facility such as NB heating system and the base support structure are to be used in the same manner as that in JT-60SC design. In this constraint, the major plasma radius cannot be changed so much, although low aspect ratio plasma is easily obtained in reduced major radius. In the first design, NCT-1, the outboard side of the toroidal field coil and vacuum vessel are extended by 50 cm in outward direction [6]. Low aspect ratio of A ~ 2.8 is achieved by increasing the minor radius a_p ~ 1.1 m. In this design, the maximum supplied flux and the maximum toroidal magnetic field are almost the same as those in JT-60SC. More improved flexibility with lower aspect ratio A ~ 2.6 is realized in the second design, NCT-2, in which the inboard side of the toroidal field coil and vacuum vessel are extended by 15 cm in inward direction. In this design, the maximum toroidal field decreases to 3 T.

Table 1 shows parameters of 2 machine design studies with different flexibility in shaping. NCT-1 has moderate shaping flexibility with higher B_T compatible with present ECCD in JT-60U. NCT-2 has higher shaping flexibility with lower B_T. Both design allow single and double null divertor operations. In order to increase the shape parameter, small plasma aspect ratio as well as large vertical elongation and high triangularity are necessary. Those conditions are satisfied in double null divertor configuration. Therefore, double null configuration is adopted for the low-A ratio plasma in both designs, NCT-1, and NCT-2.

Table 1. Comparison of the main parameters of JT-60SC and NCT.

	JT-60SC[1]	NCT-1	NCT-2
I_p (MA)	4.0	4.0	5.5
B_T (T)	3.8	3.7	3.0
R_p (m)	2.80	2.9-3.1	2.8-3.0
a_p (m)	0.85	< 1.1	< 1.1
A	> 3.3	>2.8	>2.6
κ_{95}	1.8	< 1.83	< 1.83
δ_{95}	0.35	< 0.52	< 0.52
S	< 4.1	< 5.5	< 7.0
V_p (m^3)	75	< 120	<130
Divertor	Single	Single Double	Single Double

4. Physics Investigation

4.1 Flexibility in aspect ratio and shape parameter

Figure 1 shows the typical plasma cross section of middle-A and low-A configurations for NCT-1, and NCT-2. Operational points of two designs are plotted in Fig.2 as a function of aspect ratio and shape parameter as compared with those for previous JT-60SC concept. As clearly seen in the figure, the flexibility in those parameters is remarkably extended in NCT. For medium aspect ratio of A>3.1 the shape parameter is in the range of 4-5.5, on the other hand, for low aspect ratio of A<3.0 shape parameter extends to 5-8. The enlargement of the capability in the shape parameter will contribute to extend the ideal MHD stability limit.

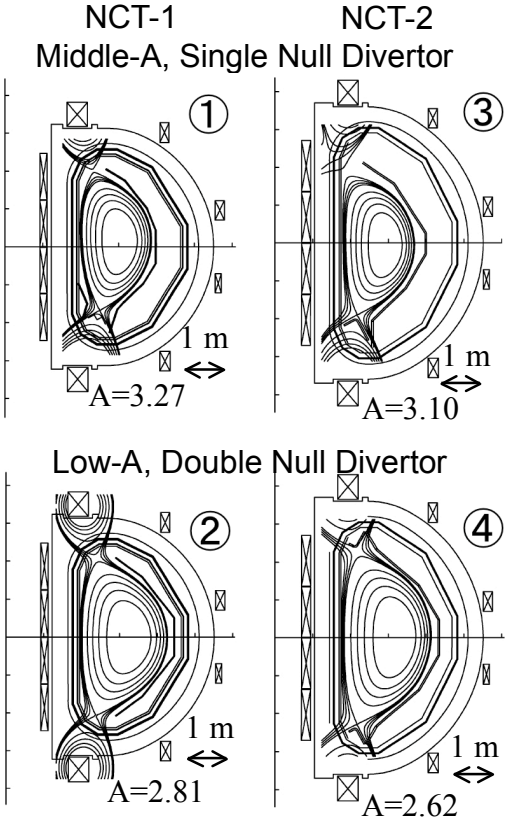

Fig.1 Typical plasma cross section of middle-A and low-A configurations for NCT-1, and NCT-2.

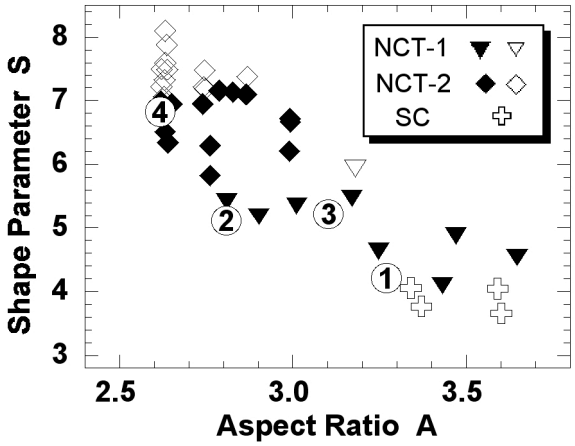

Fig.2 Operational points of two designs as a function of aspect ratio and shape parameter as compared with those for previous JT-60SC concept (IAEA2002).

As mentioned in previous section, vertical elongation is limited in order to keep the divertor pumping capability. For the control of divertor detachment the pumping speed larger than 100 m^3/s is required. In such a constraint the achievable shape parameter decreases as shown by solid symbols in the figure.

4.2 High-β plasma accessibility

Due to the constraint of the reuse of heating facility, injected power decreases with increase of pulse duration. Typical power are 44 MW, 41 MW, 30 MW, 25 MW, and 15 MW, for 10 s, 20 s, 30 s, 50 s, and 100 s, respectively. Based on the experimental achievement in JT-60U, if the improved confinement factor, $HH_{(y,2)}$ =1.5-2.0 is assumed, maximum attainable β_N is estimated as shown in Fig.3, where I_p=1.5 MA, B_T=1.8 T, and f_{GW}=0.8. Hatched area is the attainable region. In middle-A of both machine designs, high-β steady-state operation of β_N =3.5 for 100 s is achievable. On the other hand, in low-A configuration the increase of plasma volume brings the decrease of heating power density, therefore, the operation with lower

BT~1.5 T, also shown in the figure, might be considered. If the heating power of 25 MW for 100 s is assumed, the achievable β_N>4 is expected. Increase of injected power through the

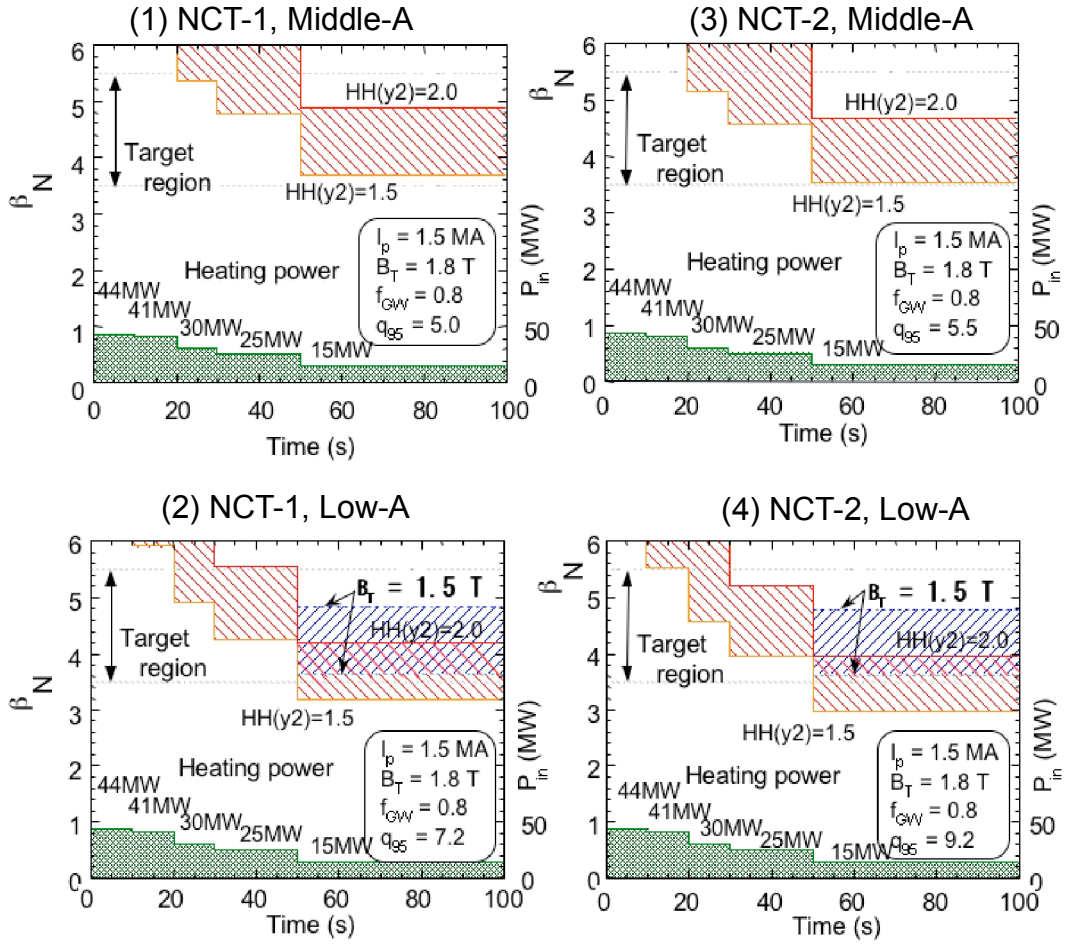

Fig.3 Achievable b_N versus heating pulse duration for middle-A, and low-A of NCT-1 and NCT-2.

improvement of beam source will be more suitable way for high β operation.

MHD stability limit for the RWM instability is compared with aspect ratio by the ERATO-J code analysis [7]. Critical β_N for n=1, and n=2 mode is plotted against the location of ideal conformal wall in Fig.4. In each case the elongation is fixed at κ_{95}=1.8, therefore, the figure indicates that the critical β_N is improved in lower aspect ratio. Advantage of low aspect ratio on the view point of MHD stability is confirmed.

In order to sustain high-β steady-state operation (β_N =3.5-5.5, for 100 s), feedback control of neoclassical tearing mode with the use of ECCD and that of resistive wall mode (RWM) with the use of in-vessel coils with ferritic wall [8] are maintained in the design.

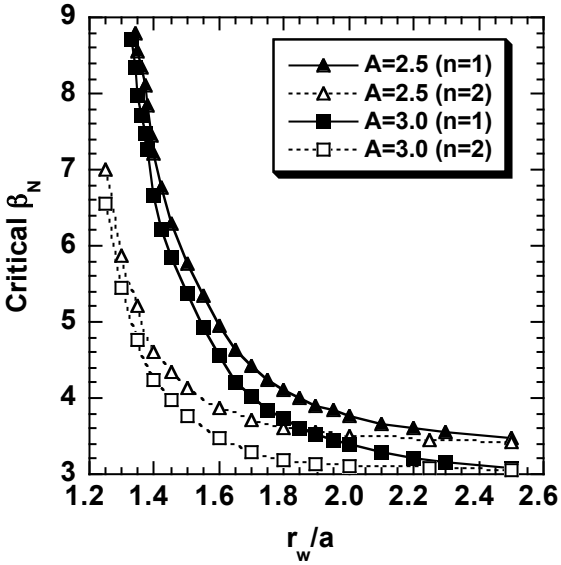

Fig.4 Critical b_N for n=1 and n=2 mode for A=2.5(triangles) and A=3.0(squares) as a function of ideal wall location (r_W/a).

The applicability of reduced-activation ferritic steel as a first wall of DEMO will be tested in this device on the basis of JFT-2M experiments [9].

4.3 Current drive controllability

By the outward shift of the toroidal field coil and vacuum vessel in NCT designs, the trajectory of NB injection might be affected. Driven current is compared for middle-A and low-A configuration using with ACCOME code analysis [10]. Dependences of current density profiles on the central electron density in high-β plasma of β_N~3.5 with I_p=3MA are shown in Fig.5. There are small differences in current profile between NCT-1 and NCT-2,

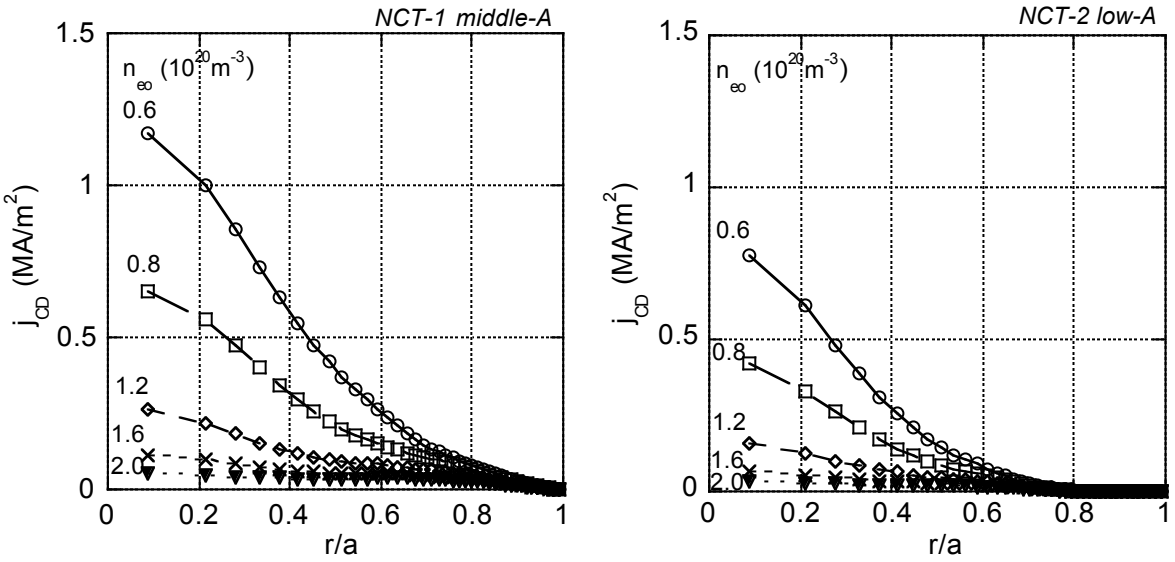

Fig.5 Current density profiles for middle-A of NCT-1, and low-A of NCT-2. Central electron densities are scanned at 0.6, 0.8, 1.2, 1.6, and 2.0 x $10^{20}m^{-3}$, respectively.

therefore, middle-A of NCT-1, and low-A of NCT-2 are shown. In both configuration, the current drive in peripheral plasma at r/a>0.6 is very small. Controllability of peripheral current drive will be contributed by bootstrap current or by additional EC or LH current drive. In the present JT-60U experimental observation [11], a bootstrap current drive profile is closely correlated with the internal transport barrier (ITB) location, and extends to r/a~0.7 in some shots. The current profile in peripheral plasma is considered to be controllable by ITB.

4.4 Break-even class plasma

Table 2 Reonance of EC

	m/n	ρ_s	I_{EC}/P_{EC} (kA/MW)	W_{EC}	P_{EC}^{min} (MW)
NCT-1 mid-A	3/2	0.53	20.5	0.049	2.2
	2/1	0.73	12.1	0.028	2.2
NCT-2 low-A	3/2	0.51	40.0	0.098	3.2
	2/1	0.71	21.0	0.038	2.0

Break-even-class plasma performance is investigated in the view point of equivalent Q_{DT}, Q_{DT}^{eq}, and the operation window of normalized Larmor radius, ρ*, and normalized collisionality, ν*. For middle-A and low-A configurations of NCT-1, NCT-2, Q_{DT}^{eq} ≥1 is achievable at I_p=4-5.5 MA, f_{GW}=0.7, P_{NB}=13 MW for 100 s, assuming $HH_{(y,2)}$=1.23, at which ρ*~10^{-3}, and ν*~10^{-1} are estimated. Those are in the range for research target of NTM

controllability with break-even class plasma.

Another concern is the EC resonance for the NTM suppression. Resonance conditions are compared between middle-A of NCT-1 and low-A of NCT-2 for normal shear plasma with q_o=1 analysed by Rutherford equation. As summrized in Table 2, the minimum EC power, P_{EC}^{min}, for the NTM stabilization with m/n = 3/2, 2/1 is 2 - 3 MW, which is available power level of present EC system, though the resonance width, W_{EC}, is slightly larger in the low-aspect ratio case of NCT-2.

Operation window of simultaneous achievement of high-Q_{DT} and high-β_N is also estimated. Plasma current and toroidal field are surveyed at NB input power of 27 MW for middle-A of NCT-1 and low-A of NCT-2, as shown in Fig.6. In the figure averaged electron density is surveyed at f_{GW}=0.5-1.0. Simultaneous achievement of β_N~4, with Q_{DT}~0.6 at I_p=3 MA, B_t=2.4 T, and f_{GW}~1 in middle-A, and of β_N~3.7, with Q_{DT}~0.7 at I_p=4 MA, B_t=2 T, and f_{GW}~1 in low-A will be expected after the increase of NB power to 27 MW.

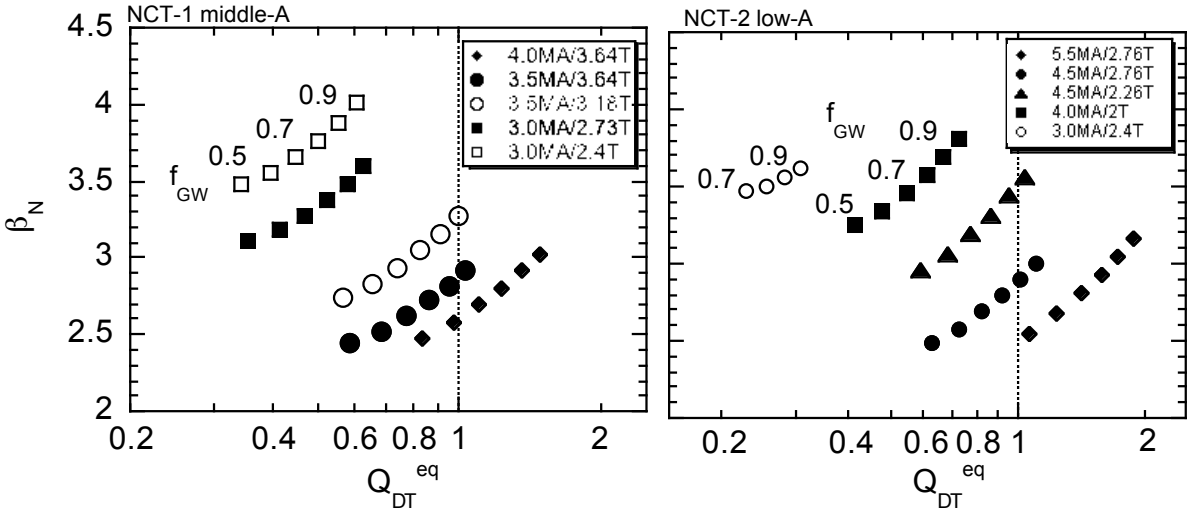

Fig.6 Operation window of simultaneous achievement of high-Q_{DT} and high-b_N with P_{NB}=27 MW.

4.5 Assessment of Day-long Operation

Demonstration of year-long operation will be required in DEMO. For such a long pulse, different physics might be important such as extreme reduction of disruption probability, effect of wall saturation on plasma performance, and control of divertor plasma compatible with year-long operation. Taking advantage of superconducting coils, feasibility of long discharge, so-called "day-long operation" is taken into account as a future option on the basis of the TRIAM-1M experiments [12]. In the day-long operation, plasma-wall interaction with a long time scale of the order of several hours could be

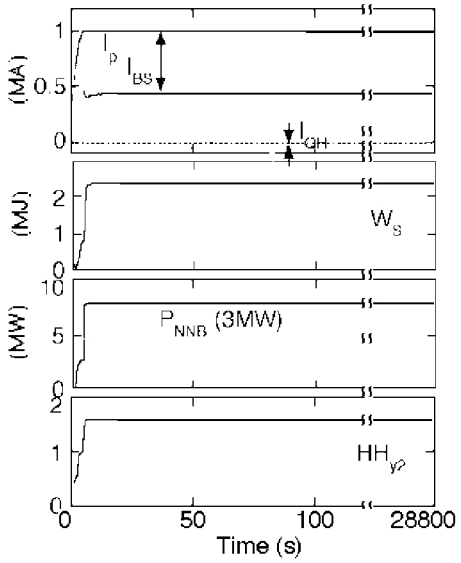

Fig.7 Typical time-trace for day-long operation simulated by the time-dependent transport code.

investigated. Fig.7 shows the typical time-trace for day-long operation simulated by the time dependent transport analysis code [13]. Steady-state condition at f_{bs}=56%, $HH_{(y,2)}$~1.6 is estimated with I_p=1 MA, B_T=1.3 T, P_{NB}= 8 MW, and f_{GW}=0.76.

5. Technology developments

Engineering design and the R&D of NCT are mainly succeeded from those developped in JT-60SC [14]. One of new development for the superconducting coils such as precise investigation on the conductor is presented in this conference [15]. Besides, the several structural designs are newly investigated. Some of them are described as follows.

5.1 Supporting structure of superconducting coils

For the supports of Central Solenoid (CS) and Divertor Coil (EF4), which suffer the large vertical forces in the single-null divertor configuration, a link structure is adopted in NCT to cancel out the vertical forces with a small moment, as shown in Fig.8 [16]. It has a continuous geometry in the toroidal direction including electrical breaks. The link structure is mounted on the TF coil, therefore, all vertical forces of the poloidal field coils are loaded on th TF coil case. In addition, it also allows the tilt of the TF coil due to the over-turning force. By adopting the link structure, the compact support structure becomes available, which contributes to reduce the resorce amount and to improve the space utility.

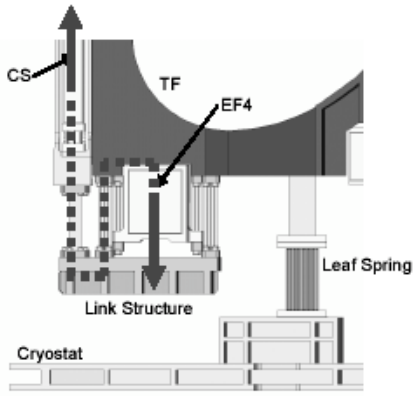

Fig.8 Support structure for superconducting coils.

5.2 Vacuum vessel (VV)

The structure of double-skin VV is illustrated in Fig.9. In order to ensure the toroidal resistivity as high as 50 μΩ for the initial plasma production, the thickness of VV is optimized as 10 mm for inner skin and 8 mm for outer skin. Water is filled in the gap for the neutron shield, while the hot N_2 gas is injected for the wall baking. C-shape support rib is connected on the outer skin by the fillet weld and on the inner skin by the plug weld for the easy maintenance.

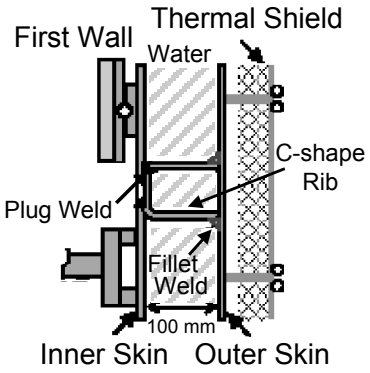

Fig.9 Vacuum vessel

5.3 Neutron shield materials

D-D neutron shield materials doping with boron are designed in the aspect of TF coil shield and bio-protection. Based on the superior characteristic in effective D-D neutron absorption and applicable temperature, boron-doped regin is developed [17] as a neutron shield around the vacuum vessel with baking

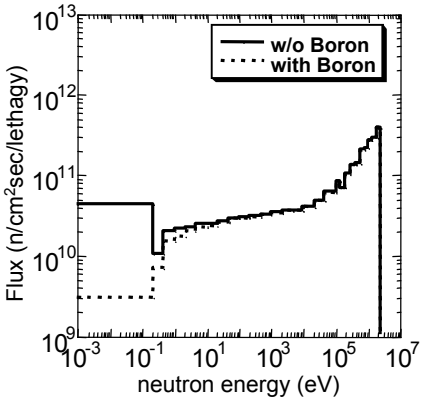

Fig.10 Energy spectra of neutron penetrating the resin shield

temperature of ~300˚C. As shown in Fig.10, thermal neutron (E < 0.2 eV), calculated by the 1D-analysis code (ANISN), is effectively absorbrd by boron, which in turn contributes to the capture of γ-ray flux with energy more than 1 MeV and to decrease the nuclear heating in TF coils. DD-neutron irradiation test with the specimen of developed resin with 2-wt% boron-doping shows the reduction in the penetration rates of thermal neutron flux as expected from the calculation.

6. Conclusions

National Centralized Tokamak facility is defined to extend the flexibility in aspect ratio and shape controllability for the demonstration of the high-β steady state operation with nation-wide collaboration. The machine design is performed with the base of previous JT-60SC design to ensure the high shape parameter of S~7 achieved by the low aspect ratio of A~2.6 as well as high elongation of κ_{95}~1.9. Low aspect ratio plasma is advantageous to extend the MHD stability limit. However, due to the present facility constraint decrease of the heating power density limits the attainable β_N in low-A configuration. Increase of NB injection power will be the key issue in high-β accessibility.

References

[1] M. Kikuchi, *et al.*, Nucl. Fusion 30 1990) 265.
[2] S. Ishida, *et al.*, Nucl. Fusion 43, (2003) 606.
[3] M. R. Wade, *et al.*, Phys. Plasmas 8 (2001) 2208.
[4] Y. Gribov, *et al.*, in 18th IAEA Fusion Energy Conference, IAEA-CN-77/ITERP/02.
[5] S. Sakurai, *et al.*, Plasma Phys. Control Fusion 44 (2002) 749.
[6] M. Matsukawa, *et al.*, IEEE Transactions of Applied Superconductivity 14 (2004) 1399.
[7] S. Tokuda, *et al.*, Rep. JAERI-M 9899, Japan Atomic Energy Research Institute, 1982.
[8] G. Kurita, *et al.*, Nucl. Fusion 43 (2003) 949, and in this Conference /FT/P7-7.
[9] K. Tsuzuki, *et al.*, this conference IAEA-CN-116/EX/P2-33.
[10] H. Tamai, *et al.*, Plasma Science & Technology 6 (2004) 2281.
[11] T. Fujita, *et al.*, Phys. Rev. Lett 8 (2001) 085001.
[12] S. Itoh *et al.*, Nucl. Fusion 39 (1999) 1257.
[13] K. Ushigusa, *et al.*, in Fusion Energy 1998 (Proc. 17th Int. Conf. Yokohama, 1998) (Vienna, IAEA) FTP/12.
[14] A. Sakasai, *et al.*, Nucl. Fusion 44 (2004) 329.
[15] K. Kizu, *et al.*, in this Conference /FT/P1-6.
[16] M. Matsukawa, *et al.*, IEEE Transaction on Appl. Superconductivity 14 (2004) 1399.
[17] A. Morioka, *et al.*, J. Nucl. Science and Technology, Suppl 4 (2004) 109.